MELTING FRONT PROPAGATION IN A PARAFFIN-BASED PHASE CHANGE MATERIAL – LAB-SCALE EXPERIMENT AND SIMULATIONS

Josef STETINA[1], Tomas MAUDER[1], Lubomir KLIMES[1,*], Pavel CHARVAT[1]

[1] Brno University of Technology, Faculty of Mechanical Engineering,
Energy Institute, Technicka 2896/2, Brno, Czech Republic

[*]Corresponding author: klimes@fme.vutbr.cz

The paper reports experimental and numerical investigation of the melting front propagation in a paraffin-based Phase Change Material (PCM). The investigated case was a block of PCM with a heat flux introduced at one of its sides. The PCM block was contained in a transparent container and thus the propagation of the melting front could be monitored with a camera. The melting temperature of the PCM was 28 °C and the container was located in an environmental chamber where the ambient temperature was maintained at 27 °C during the experiment. The natural convection in the melted PCM played an important role and it had to be considered in the heat transfer models. The numerical models taking into account natural convection in liquid PCM require long computation times, and therefore they are impractical if the fast computation of the melting front position is needed. The effective heat conductivity approach can be used to overcome this issue. Two numerical models were compared; an in-house heat transfer model using effective conductivity approach developed in MATLAB and a more advanced model created in the off-the-shelf simulation tool COMSOL, which accounts for the natural convection in liquid PCM.

Keywords*: phase change problem, phase change materials, effective thermal conductivity, melting front*

1. Introduction

The phase change of matter is a phenomenon encountered in many technical applications from metal production and processing to latent heat thermal energy storage to ice making and food freezing [1-3]. Though analytical solutions are available for specific cases of phase change problems (see e.g. [4]), numerical methods and simulations are widely used for the investigation of thermal behaviour of such systems. Several approaches can be used for numerical simulation of the problems involving the phase change of matter [5]. The selection of an appropriate numerical method is usually dependent on the definition of the problem, required accuracy, and computational demand. In general, two different classes of numerical methods can be utilized for solution of the heat transfer problems involving a phase change. The first class includes methods, which primarily solve the temperature distribution. In such case the interface between the phases is not tracked explicitly but it can be approximately determined from the temperature distribution. It means that the spatial interpolation of temperatures between the spatial nodes with the temperatures below and above the phase change temperature is

usually carried out and used for an approximate reverse determination of the interface location. Further details on this approach can be found e.g. in [6]. Such methods are called the interface capturing methods [7]. The enthalpy method mentioned in [7] is the well-known interface capturing technique. The method relies on introducing the enthalpy thermodynamic function, which includes both the sensible and latent heat. The discretized governing heat transfer equations then contain the unknown values for both the enthalpy and the temperature. The two-step solution procedure has to be used to determine the value of the enthalpy in the first step and the temperature from the enthalpy-temperature curve in the second step. This feature also makes the use of the implicit time discretization quite difficult. On the other hand, the enthalpy method is straightforward and easy for implementation.

On the other hand, the interface tracking methods primarily track the interface location, which is followed by the determination of the temperature distribution. Such methods are very precise but also computationally demanding [7]. Another problem in numerical modelling of phase change is to properly address all the phenomena, which significantly influence the behaviour of the studied case and which thus have to be considered in the model. The natural convection due to buoyancy forces is an example of the phenomenon, which can be omitted in some cases, especially when the amount of material is relatively small (e.g. microencapsulated phase change materials [8]) or when the thermal diffusivity and the viscosity are high and conduction is the dominant way of heat transfer. However, natural convection can be very important in cases with low values of thermal diffusivity and viscosity causing significant flow patterns induced by buoyancy forces. This is also the case when the geometry and other conditions allow for significant buoyancy forces (e.g. vertical cavities or containers [9, 10]).

When the detailed investigation of the fluid flow is not required, but the fluid flow still needs to be taken into account, a number of investigators utilize the concept of the effective thermal conductivity. This method is used to include the effects of the fluid flow phenomena by means of an artificial increase of the thermal conductivity for the liquid phase. Oksman et al. [11] investigated the effective thermal conductivity in computer models for continuous casting of steel. Sun et al. [12] experimentally investigated heat transfer enhancement caused by natural convection during melting of a phase change material (PCM). The PCM was enclosed in a cubic aluminium container with the dimensions 0.2 m × 0.2 m × 0.2 m. The authors observed mean heat transfer enhancement factors of 1.12 and 1.30. Calvet et al. [13] investigated the enhancement of heat transfer in macro-encapsulated phase change materials by means of intensification of the effective thermal conductivity.

The present paper reports experimental and numerical investigation of the melting front propagation in a paraffin-based phase change material (PCM). The analysis aims at the determination of the effective thermal conductivity, which is used to incorporate effects of natural convection to the heat conduction model. The main advantage of such approach is the computation speed that makes it possible to perform real-time simulations.

2. Experimental study

The main objective of the experiments was to obtain experimental data that could be used in development of the numerical models for simulation of melting front propagation. As it is difficult to monitor the propagation of the melting or solidification front in metals and other opaque materials a paraffin-based PCM was chosen for the experimental investigations. The paraffin-based PCMs are of white colour when in the solid state but they are water-like transparent in the liquid state. The basic

idea of the experiment was to monitor the melting front propagation both visually (using a camera) and with the use of temperature sensors. As the initial and boundary conditions play a significant role in the numerical simulations, the experiments were conducted in the environmental chamber. The environmental chamber available to the investigators could provide ambient temperature in the temperature range between –40 °C and 85 °C with the temperature deviations of less than 1 K even over long periods of time. The proposed set-up of the experimental investigations was as follows; the PCM was contained in a transparent container. The container with the PCM was placed in the environmental chamber where the ambient temperature was set to the lower threshold of the melting range of the PCM. Then the heat flux on one side of the container was introduced. The PCM began to melt and the propagation of the melting front was monitored. The PCM with the melting temperature of 28 °C (Rubitherm RT28HC [14]) was chosen for the initial set of experiments. The properties of the RT28HC are shown in Tab. 1. There were several reasons for selecting RT28HC. With the melting threshold at 27 °C the PCM is in the solid state at normal room temperature. On the other hand, the melting threshold was so low that it allowed for all the equipment and even the investigators to be present in the environmental chamber during the experiments. Most paraffin-based PCMs have rather wide melting temperature range – sometimes wider than 5 K. The RT28HC melts and solidifies in the temperature interval of 2 K.

Tab. 1: Properties of RT28HC

Melting area	27-29 ºC, main peak 28 ºC
Congealing area	29-27 ºC, main peak 27 ºC
Heat storage capacity ±7.5% (Combination of latent and sensible heat in a temperature range of 21 °C to 36 °C)	245 kJ
Specific heat capacity	2 kJ $kg^{-1}K^{-1}$
Density solid (15 ºC)	880 kg m^{-3}
Density liquid (40 ºC)	770 kg m^{-3}
Heat conductivity	0.2 W $m^{-1}K^{-1}$
Volume expansion	12.5%
Maximum operation temperature	50 ºC

The manufacturer delivers the PCM in plastic canisters. The canister with the PCM was placed in the environmental chamber where the temperature was maintained at 40 °C. When the PCM melted it was poured into the container shown in Fig. 1. The container was made of transparent polycarbonate sheets with the thickness of 25 mm. One of the walls of the container consisted of a 3 mm thick aluminium plate with an electric heating foil on its external side. The heating foil was powered by a precise DC power source with the output voltage adjustable in the range from 0 V to 30 V. The experiments were carried out with the voltage of 20 V. The constant voltage of the power source and the essentially constant resistance of the electric heating foil resulted into a constant electric current of 1.96 A during the experiments. The temperature of the PCM was measured with the teflon coated T-type thermocouples at 5 locations at the intersection of the horizontal and vertical mid-planes of the PCM block. The thermocouples, held in a special holder, were inserted in the PCM when it was in the

liquid state. The holder consisted of a clamp and 5 brass tubes holding the thermocouples in the defined positions. The sensing junctions of thermocouples protruded about 3 mm from the brass tubes. The thermocouples were connected to the high-accuracy thermocouple module NI 9214. The entire temperature monitoring set-up was calibrated with the use of the dry block calibrator OMEGA CL1000 in the temperature interval between 10 °C and 60 °C. As the absolute values of the measured temperatures were not as important as the differences between the readings of the individual thermocouples the goal of the calibration was to minimize the differences between the readings of thermocouples at the same dry block calibrator temperature. In this respect the uncertainty of temperature monitoring was about 0.2 K. The positions of the thermocouples are shown in Fig. 2. The NI 9219 module with four analogue channels was used for connecting the RTD (Pt100) temperature sensors. These sensors monitored the surface temperature of the heated wall of the container. The monitoring software was created in LabView 2014. Considering the slow progress of the PCM melting

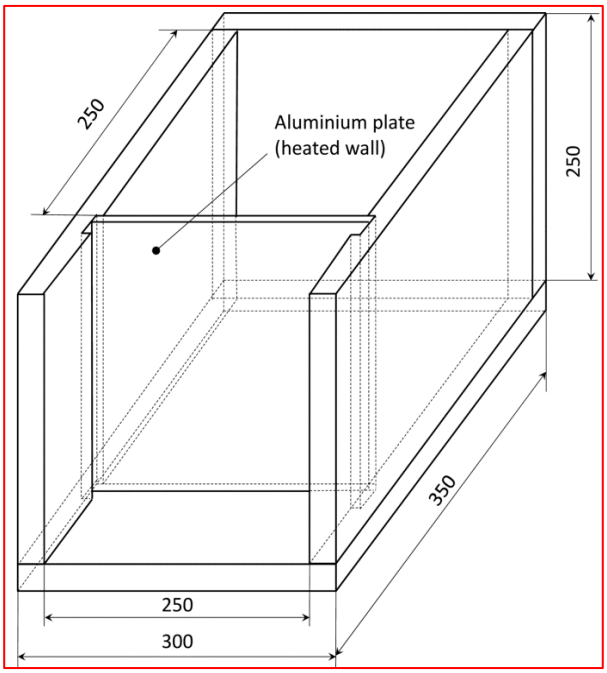

a sampling period of 60 seconds was used. The data were saved in the LVM format and further processing and evaluation of the data was done in MATLAB.

Fig. 1: Container for the PCM

The propagation of the melting front was monitored visually. The Nikon D90 camera with the Sigma macro lens was used to obtain pictures of melting front propagation. The pictures were taken in 60 second intervals. The trigger Aputure Pro Coworker II AP-WTR3N was used to synchronize photo shooting with data acquisition. As the experiments took place in the environmental chamber a LED photo flash was used for illumination. The environmental chamber had stainless steel walls that created disturbing reflections of the photo flash. For that reason the container was placed in a photo shooting tent with the opaque black background (Fig. 2). The ambient temperature in the environmental chamber was 27 °C.

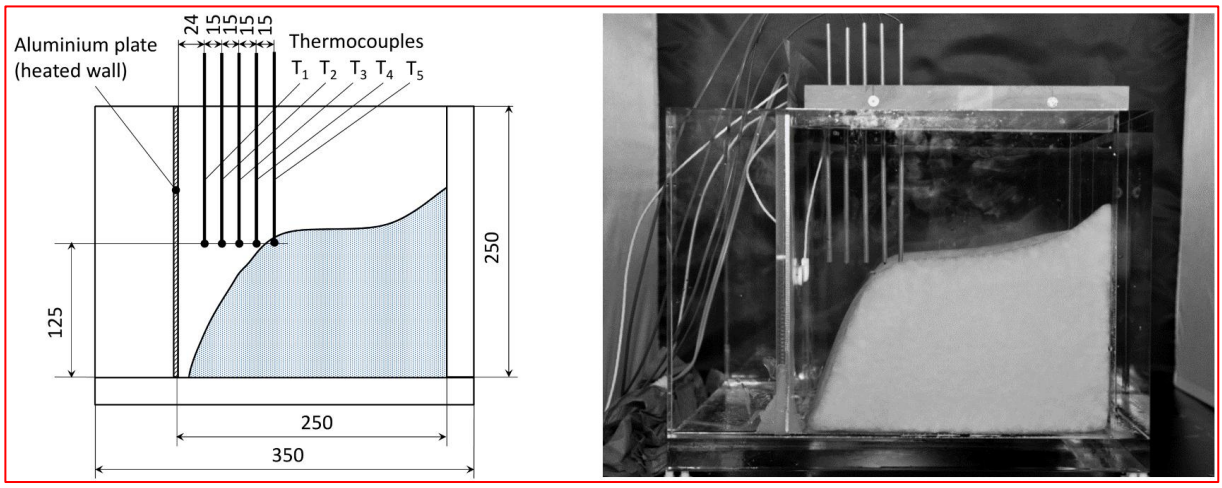

Fig. 2: Container with partially melted PCM

3. Numerical simulations

The aim of the numerical simulations was to investigate the accuracy of two models utilizing the effective heat capacity approach [15] in dealing with the phase change. The first model was created in the off-the-shelf commercial software COMSOL. It was a two-dimensional heat and mass transfer model and it accounted for natural convection in the liquid PCM. Laminar flow was considered in this case. The second one was an in-house heat transfer model implemented in MATLAB. The model was formulated as two-dimensional heat transfer model and it accounted for effects of natural convection by means of an approximate approach via the effective thermal conductivity.

Both models adopted effective heat capacity method to account for latent heat. The Gausian-like relation between temperature and effective heat capacity, which is often adopted by researchers (see e.g. [16-18]), was used as described by the following equation

$$c_{\mathrm{eff}}(T) = c_0 + c_{\mathrm{m}} \exp\left\{-\frac{\left(T - T_{\mathrm{pch}}\right)^2}{\xi}\right\} \tag{1}$$

where T [K] is the temperature, c_0 [J kg^{-1} K^{-1}] is the specific heat, c_{m} [J kg^{-1}K^{-1}] is the maximum increment of the specific heat due to the latent heat and ξ [K^2] is the parameter influencing the width of the phase change temperature interval. The mean temperature of phase change T_{pch} [K] for melting and congealing was considered to be T_{pch} = 301.15 K (28 °C), the specific heat c_0 = 2000 J kg^{-1}K^{-1}, the maximum increment of the specific heat due to the latent heat c_{m} = 252 880 J kg^{-1}K^{-1} and ξ = 0.23 K^2. The effective capacity curve is shown in Fig. 3 where the solidus temperature T_S and the liquidus temperature T_L are 27 °C and 29 °C, respectively.

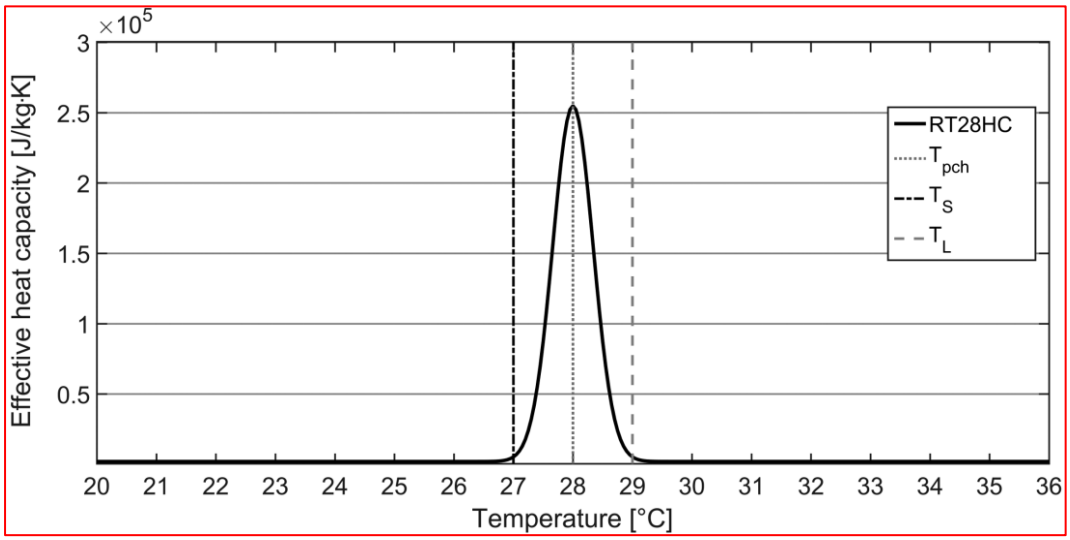

Fig. 3: Effective heat capacity

3.1. 2D heat transfer and fluid flow simulation in COMSOL

The experimental results confirmed a significant influence of natural convection in the melted PCM. Natural convection occurred due to the variation of density of the melted PCM in the vertical direction. The variation in density induces the buoyancy force that is the driving force of natural convection. Natural convection in the liquid PCM considerably enhanced the heat transfer rates between the liquid and solid PCM. The multi-physics FEM modelling tool COMSOL allows for the coupled heat transfer and fluid flow simulations. Such a coupled model makes it possible to simulate melting of PCM with much more realistic results than in case of the heat transfer simulation only. Several studies into melting and solidification of PCM carried out in COMSOL have been published, e.g. [19]. The phase change of the PCM was modelled with the use of the effective heat capacity method [20]. The coupled heat transfer and fluid flow transient problem is described with the heat transfer equation

$$\rho c_{\text{eff}} \frac{\partial T}{\partial t} = \nabla \cdot \left(k \nabla T\right) + \rho c_{\text{eff}} \vec{u} \cdot \nabla T \tag{2}$$

and the Navier-Stokes equation for the incompressible fluid flow

$$\rho \frac{\partial \vec{u}}{\partial t} + \rho\left(\vec{u} \cdot \nabla\right)\vec{u} = \nabla \cdot \left(- p\vec{I} + \mu\left(\nabla \vec{u} + \left(\nabla \vec{u}\right)^{T}\right)\right) + \rho \vec{g} \tag{3}$$

with the continuity equation

$$\rho \nabla \cdot \vec{u} = 0. \tag{4}$$

The last term ρg in the Navier-Stokes equation (3) represents buoyancy forces induced with distinct density. The heat transfer equation (2) and the Navier-Stokes equation (3) are coupled together in COMSOL by means of the non-isothermal flow interface. The COMSOL utilizes the finite element

method and the simulation was carried out for the mapped quadrilateral mesh with about 1000 elements.

3.2. An in-house 2D heat transfer model

The developed in-house 2D numerical model directly addressed only heat transfer in the PCM and not the fluid flow (mass transfer). The methodology how to include the influence of the convective part of heat transfer in the governing equation Eq. (2) and the fluid flow effects into the in-house model was devised by means of the modified effective thermal conductivity described below. The governing equation of heat transfer is in the form of

$$\rho c_{\text{eff}} \frac{\partial T}{\partial t} = \nabla \cdot \left(k_{\text{eff}} \nabla T \right) \tag{5}$$

where

$$k_{\text{eff}} = k_{\text{s}} f_{\text{s}} + A k_{\text{l}} \left(1 - f_{\text{s}} \right) \tag{6}$$

is the effective thermal conductivity and

$$f_{\text{s}} = \frac{T_{\text{l}} - T}{T_{\text{l}} - T_{\text{s}}} \tag{7}$$

is the solid fraction representing the ratio between the solid and liquid phases. The parameter A [-] is proportional to the convective term of heat transfer and it accounts for the fluid flow effects. For A = 1, there is no enhancement of heat transfer due to convection and fluid flow in the mushy or liquid phase region. The dependence between the parameter A and the Nusselt number can be written as [21, 22]

$$A = \frac{Q_{\text{convection}}}{Q_{\text{conduction}}} = \text{Nu} \tag{8}$$

Melting of the PCM in the container is a complex heat transfer process that involves both conduction and advection. As the motivation behind the 2D in-house model was to develop a simple tool for fast simulations with acceptable accuracy, the model, contrary to CFD models, does not account for advection. An approach of the effective heat conductivity was adopted in the model in which the contribution of advection to heat transfer is incorporated in the effective thermal conductivity of PCM in the liquid state. The effective thermal conductivity was considered only as a function of y-axis. The average Nusselt number was calculated from the modified empirical formula [23]

$$\text{Nu} = 0.42 \left(n \frac{\text{Ra}(y)}{\text{Ra}(H)} \right)^{1/4} \text{Pr}^{0.012} \left(\frac{H}{L} \right)^{-0.3} \tag{9}$$

where Ra is the Rayleigh number as a function of vertical position y [m],

$$\text{Ra}(y) = \frac{g\beta(T_{\text{wall}} - T_{\text{m}}) y^3}{\alpha \nu} \tag{10}$$

Pr [-] is the Prandtl number, H [m] and L [m] are characteristic dimensions of the melted PCM, g [m s^{-2}] is the standard gravity, β [K^{-1}] is the volumetric thermal expansion coefficient, T_{wall} [K] is the temperature of the heated wall, T_{pch} [K] is the mean phase change temperature of the PCM, α [m^2 s^{-1}] is the thermal diffusivity, υ [m^2 s^{-1}] is the kinematic viscosity and n [-] is the coefficient of the increase of thermal conductivity due to convection. The explicit finite differences were employed to discretize the in-house numerical model on the Cartesian uniform grid with 62 500 nodes. The time step of 1 second was chosen according to the stability condition [23].

3.3. Initial and boundary conditions

The initial and boundary conditions applied in computer simulations were obtained from the experiment. The temperature distribution at the beginning of the simulation (initial condition) through the computational domain was taken as an interpolation between thermocouple measurement at the time t = 0 for both models. The Dirichlet and Robin boundary conditions (11) and (12) were used at the boundary of the spatial domain

$$T(x,y)\big|_{x=0} = T_{\text{heater}}(t) \tag{11}$$

$$\dot{q}(x,y) = \frac{1}{\dfrac{1}{h_{\text{out}}} + \dfrac{d_{\text{wall}}}{k_{\text{wall}}}}\left(T_{\text{amb}} - T_{\text{surface}}(t)\right) \quad \text{for} \quad (x = x_M, y), (x, y = 0), (x, y = y_N) \tag{12}$$

where $\dot{q}$ [W m^{-2}] is the heat flux, M is the index of the last node in the direction of the x axis (x_M = 250 mm) and N is the index of the last node in the direction of the y axis (y_N = 250 mm). The ambient temperature was T_{amb} = 27 °C, the heat transfer coefficient was h_{out} = 5 W m^{-2}K^{-1}, the thickness of the wall was d_{wall} = 0.025 m and its thermal conductivity was k_{wall} = 0.18 W m^{-1}K^{-1}. The temperature of the heated wall was a time-dependent variable $T_{\text{heater}}(t)$. The measured values of the $T_{\text{heater}}(t)$ (see Fig. 4) were used as input in the simulation.

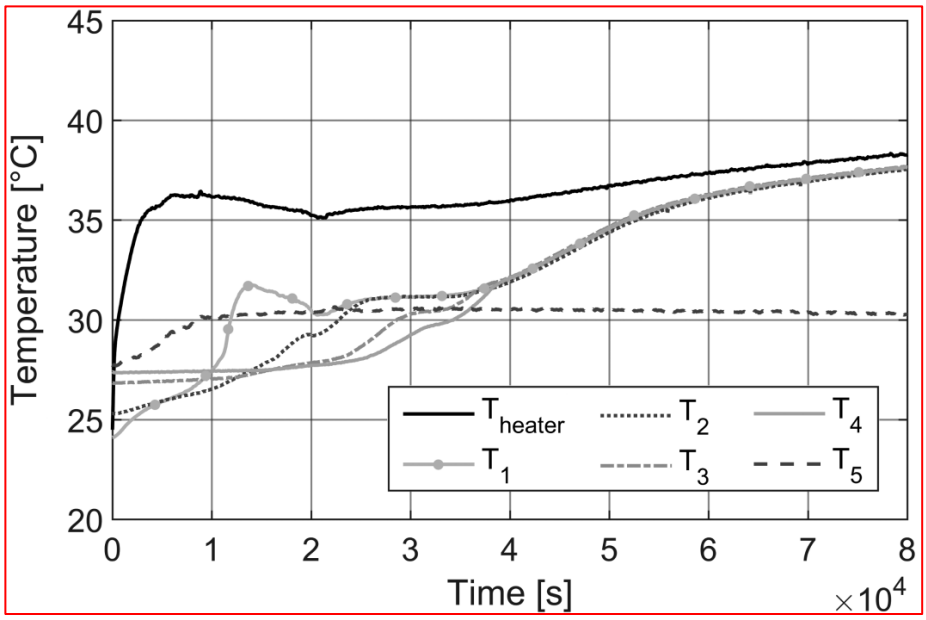

Fig. 4: Temperature distributions from measurement

Fig. 4 shows the temperatures recorded in the experiment displayed in Fig. 2. As can be seen, the initial temperature of the PCM was not uniform in the entire volume at the beginning of the experiments. In order to bring the PCM to the solid state the temperature in the environmental chamber was kept at 15 °C and only before the experiment it was increased to 27 °C. As a result the initial temperature of the PCM at the location of the thermocouple T_1 (one closest to the wall of the container) was the lowest and the temperature at the location of the thermocouple T_5 the highest. The surface temperature of the heated wall T_{heater} increased rather quickly when the heater was switched on at time t = 0 s. It was because the PCM was in the solid state and the heat flux could only be transferred to PCM by conduction. As the PCM melted the heat flux was transferred from the surface by convection. As the power supplied to the heater was constant (39 W) throughout the experiment the surface temperature of the heated wall T_{heater} increased – the temperature of melted PCM increased and as the result the surface temperature of the heated wall increased as well. The temperature of the melted PCM at the position of thermocouples T_1, T_2, T_3 and T_4 was almost the same from the time of about 40 000 s as a result of intensive mixing due to natural convection. The temperature at the location of thermocouple T_5 does not change very much as the thermocouple was buried in the solid PCM during the entire experiment as can be seen in the photo in Fig. 2. The increasing temperature of the melted PCM translated into higher thermal loss to the surrounding environment, which was maintained at 27 °C. As a result it was not possible to melt the entire volume of the PCM.

4. Results and discussion

The experimental and numerical results of the melting front propagation with the ratio between the solid and liquid states are shown in Fig. 5. The results are shown for three elapsed times. As can be seen, natural convection in the liquid PCM has a significant influence on the propagation of the melting front. Warm liquid PCM from the vicinity of the heated wall was rising up due to the buoyancy forces and thus the melting front propagated much quicker at the top of the container. The COMSOL model was able to account for this behaviour very well due to the complex modelling approach. The in-house heat transfer model was also able to account for effects of the natural convection and fluid flow quite well by using effective heat conductivity approach. In the investigated case the average value of the parameter A according to the horizontal position was determined to be A = 25.08. However, it has to be pointed out that for a different configuration the value of the parameter A has to be re-evaluated and verified with an experiment. The use of the simple in-house model as a versatile simulation tool is therefore quite limited due to this reason.

The ratios between the solid and liquid phases are shown in Fig. 5 and it can be seen that both the models provide results of the heat transfer with phase change which are in a good agreement with the experimental data. As for the shape and location of the phase interface, the results acquired with the use of the COMSOL model are in a better agreement with the experimental data since the COMSOL model accounts for a detailed fluid flow while the in-house model uses a simplified approach. However, the in-house model still provides a good and realistic approximation of the phase interface. On the other hand, the coupled multi-physics simulation in COMSOL required a significantly longer computational time in comparison to the in-house heat transfer model. In particular, a computer with two processors having 32 cores and 128 GB RAM memory was used as the hardware for simulations. The COMSOL model required about 2 seconds of computational time for 1 second of the wall-clock time. In case of the in-house code, simulation of 1 second of the wall-

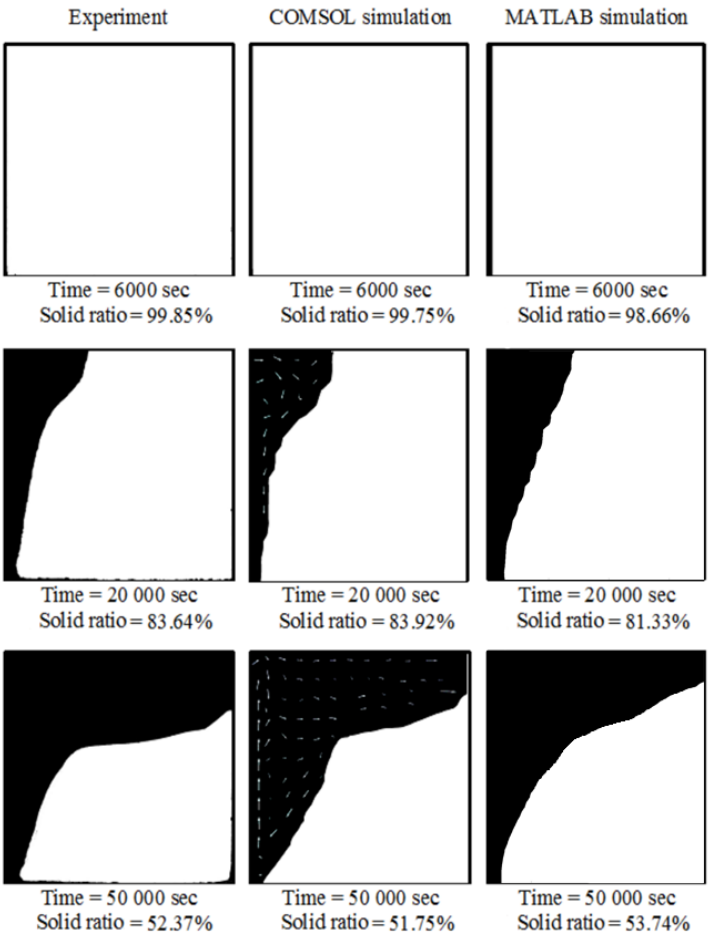

Fig. 5: Melting front propagation (liquid phase: black colour, solid phase: white colour)

clock time required just about 0.02 seconds of the computational time. Thus, the computational time of the in-house model was about one hundred times shorter than in case of the COMSOL model.

5. Conclusion and future work

An experimental and numerical study into the melting front propagation in a PCM was carried out. The goal of the experiments was to obtain data for validation of the numerical models. The experiments with high repeatability of the achieved results are needed for this purpose. This requires both a well-defined problem and the methodology for its accurate monitoring. Two models employing the effective capacity method were used for simulation of the experiment. The combined 2D heat transfer and fluid flow model created in COMSOL was able to predict the melting front propagation rather accurately. The discrepancies originated mainly from the lack of knowledge of the material properties of the RT28HC, namely the dependence of density and viscosity on the temperature. The in-house 2D heat transfer model accounted for natural convection and fluid flow by means of the effective thermal conductivity. Results showed that the simple in-house model provides results that are sufficiently accurate for practical application. While COMSOL, as a versatile simulation tool, allows modelling of various kinds of problems, in certain situations (e.g. for predictive control of a thermal energy storage system) a much simpler simulation model can be adopted. Such a model can be fine-tuned with the experimental data and implemented in the control software where it can utilize the boundary conditions obtained on-line from the monitoring system of thermal energy storage.

Acknowledgment

This work was supported by the Czech Science Foundation under contract No. 15-11977S "An adaptive front-tracking method for parallel computing of phase change problems".

Nomenclature

Latin letters

c	[J kg^{-1}K^{-1}]	heat capacity
f	[–]	solid fraction
g	[m s^{-2}]	standard gravity
h	[W m^{-2}K^{-1}]	heat transfer coefficient
k	[W m^{-1}K^{-1}]	thermal conductivity
p	[Pa]	pressure
Q	[W]	heat transfer rate
t	[s]	time
T	[K]	temperature
u	[m s^{-1}]	velocity

Subscripts

amb	ambient
eff	effective
l	liquid
L	liquidus
M	index of last node in x axis
N	index of last node in y axis
out	outer
s	solid
S	solidus

Greek letters

α	[m^2 s^{-1}]	thermal diffusivity
β	[K^{-1}]	volumetric thermal expansion coefficient
ρ	[kg m^{-3}]	density
μ	[Pa s]	dynamic viscosity
ν	[m^2 s^{-1}]	kinematic viscosity

References

[1] Wang, Z. F., *et al.*, Inverse problem-coupled heat transfer model for steel continuous casting, *Journal of Materials Processing Technology*, *214* (2014), 1, pp. 44-49.

[2] Wang, K., *et al.*, Modeling dendrite growth in undercooled concentrated multi-component alloys, *Acta Materialia*, 61 (2013), 11, pp. 4254-4265.

[3] Zhou, D., *et al.*, Review on thermal energy storage with phase change materials (PCMs) in building applications, *Applied Energy*, 92 (2012), 1, pp. 593-605.

[4] Tarzia, D. A., Relationship between Neumann solutions for two-phase Lamé-Claypeyron-Stefan problems with convective and temperature boundary conditions, *Thermal Science*, in press, doi: 10.2298/TSCI140607003T

[5] Lewis, R. W., Ravindren, K., Finite element simulation of metal casting, *International Journal for Numerical Methods in Engineering*, 47 (2000), 1-3, pp. 29-59.

[6] Stetina, J., *et al.*, Final-structure prediction of continuously cast billets, *Materiali in tehnologije*, 46 (2012), 2, pp. 155-160.

[7] Li, C. Y., *et al.*, A fixed-grid front-tracking algorithm for solidification problems. Part I – Method and validation, *Numerical Heat Transfer B*, 43 (2003), pp. 117-141

[8] Snoeck, D., *et al.*, Encapsulated phase change materials as additives in cementitious materials to promote thermal comfort in concrete constructions, *Materials and Structures*, 49 (2016), pp. 225-239

[9] Liu, H., Awbi, H. B., Performance of phase change material boards under natural convection, *Building and Environment*, 44 (2009), pp. 1788-1793

[10] Ranjbar, A. A., *et al.*, Numerical heat transfer studies of a latent heat storage system containing nano-enhanced phase change material, *Thermal Science*, 15 (2011), pp. 169-181

[11] Oksman, P., *et al.*, The effective thermal conductivity method in continuous casting of steel, *Acta Polytechnica Hungarica*, 11 (2014), pp. 5-22

[12] Sun, X., *et al.*, Experimental observations on the heat transfer enhancement caused by natural convection during melting of solid–liquid phase change materials (PCMs), *Applied Energy*, 162 (2016) 1453–1461.

[13] Calvet, N., *et al.*, Enhanced performances of macro-encapsulated phase change materials (PCMs) by intensification of the internal effective thermal conductivity, *Energy*, 55 (2013), pp. 56-964

[14] Rubitherm GmbH website. <http://www.rubitherm.de/> [accessed 27. 8. 2015; under the topic: Products, Rubitherm RT].

[15] Morgan, K., *et al.*, Improved algorithm for heat-conduction problems with phase-change, *International Journal for Numerical Methods in Engineering*, 12 (1978), 7, pp. 1191-1195.

[16] Kuznik, F., *et al.*, Energetic efficiency of room wall containing PCM wallboard: A full-scale experimental investigation, *Energy and Buildings*, 40 (2008), pp. 148-156

[17] Selka, G., *et al.*, Dynamic thermal behaviour of building using phase change materials for latent heat storage, *Thermal Science*, 19 (2015), pp. S603-S613

[18] Hed, G., Bellander, R., Mathematical modelling of PCM air heat exchanger, *Energy and Buildings*, 38 (2006), pp. 82-89

[19] Samara, F., *et al.*, Natural convection driven melting of phase change material: comparison of two methods, *Proceedings, The 2012 COMSOL Conference*, Boston, 2012.

[20] Stefanescu, D. M., *Science and Engineering of Casting Solidification*, Second edition, Springer, New York, USA, 2010.

[21] Taheri, P., Natural convection heat transfer, in: *Engineering Thermodynamics and Heat Transfer*, Simon Fraser University.

[22] Hadgu, T., *et al.*, Comparison of CFD Natural Convection and Conduction-only Models for Heat Transfer in the Yucca Mountain Project Drifts, *Proceedings*, ASME 2004 Heat Transfer/Fluids Engineering Summer Conference, Charlotte, USA, 2004, pp. 223-232

[23] Incropera, F. P., *et al.*, *Principles of Heat and Mass Transfer*, Seventh edition, Wiley, New York, USA, 2013.